Contents lists available at ScienceDirect

Micron

journal homepage: www.elsevier.com/locate/micron

Automated patterning and probing with multiple nanoscale tools for singlecell analysis

Jiayao Li^{a,*}, Yeonuk Kim^a, Boyin Liu^a, Ruwen Qin^b, Jian Li^c, Jing Fu^{a,*}

^a Department of Mechanical and Aerospace Engineering, Monash University, Clayton, VIC 3800, Australia

^b Department of Engineering Management and Systems Engineering, Missouri University of Science and Technology, Rolla, MO 65409, USA

^c Monash Biomedicine Discovery Institute, Department of Microbiology, Monash University, Clayton, VIC 3800, Australia

ARTICLE INFO

Keyword: Focused ion beam Atomic force microscopy Automation

ABSTRACT

The nano-manipulation approach that combines Focused Ion Beam (FIB) milling and various imaging and probing techniques enables researchers to investigate the cellular structures in three dimensions. Such fusion approach, however, requires extensive effort on locating and examining randomly-distributed targets due to limited Field of View (FOV) when high magnification is desired. In the present study, we present the development that automates 'pattern and probe' particularly for single-cell analysis, achieved by computer aided tools including feature recognition and geometric planning algorithms. Scheduling of serial FOVs for imaging and probing of multiple cells was considered as a rectangle covering problem, and optimal or near-optimal solutions were obtained with the heuristics developed. FIB milling was then employed automatically followed by downstream analysis using Atomic Force Microscopy (AFM) to probe the cellular interior. Our strategy was applied to examine bacterial cells (*Klebsiella pneumoniae*) and achieved high efficiency with limited human interference. The developed algorithms can be easily adapted and integrated with different imaging platforms towards high-throughput imaging analysis of single cells.

1. Introduction

The emergence of nanotechnology in recent years has provided unlimited possibilities to acquire structural and chemical maps of cells at unprecedented resolution (De Jonge and Ross, 2011; Malucelli et al., 2014; Goldstein et al., 2012). Nanoscale analytical tools, typically originated from material science, have been actively translated to the biomedicine field. For example, atomic force microscopy (AFM) has been employed to probe the surface of single cells to obtain topological and mechanical signatures (Dufrene et al., 2013; Muller and Dufrene, 2008). Modulus data obtained from tissue samples by AFM also provide an additional insight to that of conventional pathological analysis for cancer patients (Plodinec et al., 2012; Cross et al., 2007). By collecting the secondary ions generated from the target surface, secondary ion mass spectrometry (SIMS) previously limited to material research, now allows mapping of different chemical species on the cell surface with a resolution approaching 100 nm (Musat et al., 2012; Kraft et al., 2006; Utlaut, 2014).

Recently, nanoscale surface milling on cells has become feasible with Focused Ion Beam (FIB) aiming for structural and chemical imaging of cellular interiors (Heymann et al., 2006; Heymann et al., 2009;

* Corresponding authors. *E-mail addresses*: jiayao.li@monash.edu (J. Li), jing.fu@monash.edu (J. Fu).

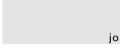
http://dx.doi.org/10.1016/j.micron.2017.06.002

Received 27 February 2017; Received in revised form 5 June 2017; Accepted 5 June 2017 0968-4328/ © 2017 Elsevier Ltd. All rights reserved.

Rigort et al., 2012). The concept is to employ highly focused ions as a 'nano-scalpel' to precisely cut the target cell. Subsequently, downstream applications including Synchrotron X-ray, SIMS and Atom Probe To-mography (APT) can then be executed (Szakal et al., 2011; Narayan et al., 2012; James et al., 2013). The cells were prepared primarily with a freeze drying protocol followed by transferring to different instruments for patterning, and the cellular compositions were expected to be preserved to a large extent (Szakal et al., 2011). Ion beam induced damage is also considered to be minimal, as suggested by simulations and previous experiments (Bassim et al., 2012). Iteratively using FIB patterning and AFM probing allows unique three dimensional investigations of the interior of cells and tissues (Liu et al., 2014; Chan et al., 2009), and cellular chemistry or delivered drugs/molecules in any arbitrary subcellular location can be probed with carefully planned patterning and probing.

To date, a tremendous amount of effort is required each time to perform the 'pattern and probe' approach enabled with FIB and other analytical techniques for single cells. High precision, as one of the preferred characteristics, is attained by limiting the pixel/step size during patterning and downstream analysis (Inkson et al., 2001). Typically the corresponding Field of View (FOV) can only cover a very

MICIOII





CrossMark

limited number of cells (Goldstein et al., 2012). Due to the random nature of biological samples, each individual cell needs to be recognized, and tedious manual selection and operation are constantly required for multiple cells. This challenge results in a significant low throughput of this novel approach (Goldstein et al., 2012), and also prevents acquiring data from a large population for statistical comparisons. The aim of the present study is to develop a platform based on the newly proposed cellular milling approach to perform automated 'pattern and probe' for single cell analysis. After initial imaging of the sample with scanning electron microscopy (SEM), feature recognition algorithm is utilized to identify the target cell. Geometric planning of patterning and probing is then executed through mathematical modelling and optimization algorithms. We demonstrate the first prototype system by automatically probing a population of drug-resistant bacterial strain (*Klebsiella pneumoniae*).

2. Materials and methods

2.1. Feature recognition of target cells

The proposed algorithm was applied to examine bacterial cells (K. pneumoniae), and the details of the sample preparation protocols were reported previously (Liu et al., 2014). Considering that only the prepared cells are the subjects of milling, areas containing cells should be precisely segmented from background for subsequent planning scheme. Upon acquiring the initial SEM image, single bacterial cells on solid substrate were identified first with the sufficient resolution provided and signal-to-noise to acquire the geometric coordinates. Gaussian filter was first applied to reduce the noise level. The standard deviation for creating the filter kernel was set to 1. A unique transformation kernel was generated for each of the input images. Entry value of the filter kernel was determined by the equation of 2D Gaussian function: $G(x, y) = \frac{1}{2\pi\sigma^2}e^{-\frac{x^2+y^2}{2\sigma^2}}$, where x and y refer to the position of entry in relation to the center entry (Hanumantharaju et al., 2013; Guo, 2011). Smoothing was then achieved by convolving the image with the computed kernel. Semi-automatic edge detection with Sobel operator was chosen to detect both step and gradual change in intensity. Three by three kernels were used: $G_x = \begin{bmatrix} 1 & 2 & 1 \\ 0 & 0 & 0 \\ -1 & -2 & -1 \end{bmatrix}$ and $G_y = \begin{bmatrix} 1 & 0 & -1 \\ 2 & 0 & -2 \\ 1 & 0 & -1 \end{bmatrix}$ (Ferreira and Rasband, 2012; Maini and Aggarwal, 2009). The input image was convolved with the above two kernels, and vertical and horizontal derivatives were approximated. Final images were obtained by replacing the pixels with the computed square root on the sum of G_x and G_v. Manual thresholding was also performed in parallel to visually confirm the recognition of cells. Without loss of generality, the geometric coordinates of the final polygons which represented the cells were exported for geometric planning (Fig. 1a).

2.2. Geometric planning and optimization

For most imaging and fabrication instruments, FOV is defined as a bounded region, a typical rectangle shape (bounding box), covered by electron/ion beam scanning or AFM cantilever probing without stage movement. The size of FOV is controlled by the aperture and control units of the instruments, and a larger size FOV (lower magnification) is usually chosen for larger features if lower resolution is acceptable (Utlaut, 2014; Giannuzzi, 2006). An FOV of reduced size is required for patterning or scanning at higher resolution. Different from the polygon covering problem encountered in the mask-making process of integrated-circuit manufacture which requires partition of a large target polygon (Reckhow and Culberson, 1987; Cheng and Lin, 1989; Hegedüs, 1982; Lubiw, 1990; Franzblau and Kleitman, 1984), an individual polygon that represents single cell is presumably coverable by one single rectangle (FOV) for most milling or probing applications. Hence decomposition of individual polygon in previous studies is not applicable in this research. To probe a population of recognized cells, the primary challenge for automation is to find an optimal series of bounding boxes, equivalent to the FOVs, to cover the target cells with predetermined resolution (Fig. 1b). The mathematical models are formulated as follows:

Let $B \subset R^2$ be a bounding box, and without loss of generality, it can be expressed as

$$B = \left\{ (x, y) \in \mathbb{R}^2: -\frac{a}{2} \le x \le \frac{a}{2}, -\frac{b}{2} \le y \le \frac{b}{2} \right\}$$
(1)

where a and b refer to its length and width, respectively. A finite number of polygons from the recognized cells are represented as

$$K_i = \{ \bigcup_{k=1}^{l_k} (x_{ik}, y_{ik}) \in \mathbb{R}^2 \}, \quad i \in I_n = \{1, 2, ..., n\}$$
(2)

where the union of points (x_{ik}, y_{ik}) are the points contouring the shape of polygon K_i ; n is the total number of polygons to be covered. For each polygon K_i , the vertices are defined as $\{(x_{i1}, y_{i1}), (x_{i2}, y_{i2}), ..., (x_{ik}, y_{ik}), ..., (x_{ilk}, y_{ilk})\}$. Since both translation and rotation are considered, a 1-by-3 transformation vector u is set up, with three entries (θ, p_x, p_y) :

$$u = \{(\theta_i, p_{xi}, p_{yi}): i \in I_n = \{1, 2, ..., n\}\}$$
(3)

where θ_i , p_{xi} , p_{yi} refer to angle of rotation, horizontal translation and vertical translation, respectively. A feasible solution u_i exists if polygon K_i is covered by bounding box B. For $x \neq y$, multiple polygons can be possibly contained in a same transformed bounding box $(u_x = u_y)$. By introducing u_i , the set for bounding box B updates to:

$$B = \{B_j | (x', y') \in R^2 : j \in I_m = \{1, 2, ..., m\}\}$$
(4)

Where B_j is the transformed bounding box for each transforming T_j ; *m* is the total number of transformation. For $x \neq y$, $B_{j_x} \neq B_{j_y}$ which means that these two transformed bounding boxes are located in different positions. Each bounding box is assumed to be distinct in terms of its geometry position. The aim is to transform the given bounding box to cover all the required polygons with the *minimized* number of transformations m, which is equivalently to fulfil the following equation:

min m

subject to:
$$(\bigcup_{i=1}^{m} B_i) \cap (\bigcup_{i=1}^{n} K_i) = (\bigcup_{i=1}^{n} K_i)$$
 (5)

The geometric planning is governed by the derived transformation u_i . Since only two-dimensional motion is concerned, the relationship between the original coordinate vector (x, y) and transformed vector (x', y') is expressed in the following equation:

$$\begin{bmatrix} x'\\ y'\\ 1 \end{bmatrix} = T\begin{bmatrix} x\\ y\\ 1 \end{bmatrix} = \begin{bmatrix} \cos(\theta) & -\sin(\theta) & p_x\\ \sin(\theta) & \cos(\theta) & p_y\\ 0 & 0 & 1 \end{bmatrix} \begin{bmatrix} x\\ y\\ 1 \end{bmatrix}$$
(6)

where **T** is the transformation matrix made by a 3-by-3 matrix. θ , p_x and p_y are the components of transformation vector **u** as defined in Eq. (3). A subscript *j* on transformation matrix **T**, represented as T_j , refers to *j*-th transformation matrix and bounding box B_j . This set covering problem is also equivalent to transforming polygons into a bounding box centred at the origin (Fig. 1b). In this case, the inverse matrices \mathbf{T}^{-1} determine the actual stage movements.

It is evident that a polygon can be covered if all its vertices are covered with the bounding box after transformation. The transformed vertices (x', y') should satisfy the following inequalities:

$$x' = |(\cos\theta)x - (\sin\theta)y + p_x| \le \frac{a}{2}$$
(7)

$$y' = |(\sin\theta)x + (\cos\theta)y + p_y| \le \frac{b}{2}$$
(8)

Download English Version:

https://daneshyari.com/en/article/5456954

Download Persian Version:

https://daneshyari.com/article/5456954

Daneshyari.com